Adjusting resonant wavelengths and spectral shapes of ring resonators using a cladding SiN layer or KOH solution

Sahnggi Park,* Kap-Joong Kim, Jong-Moo Lee, In-Gyoo Kim, and Gyungock Kim

Electronics and Telecommunications Research Institute, 161 Gajong-dong, Yusong-gu, Daejeon, 305-350, Korea
**sahnggi@etri.re.kr*

Abstract: It is shown that the resonant frequencies and the transmission spectra of ring resonators can be adjusted by depositing or etching the cladding nitride layer on the ring waveguide without introducing an extra loss or extra variations of channel spacing. The cladding nitride layer increases the minimum width of the gap in the coupling region to larger than 150nm which makes it possible to consider photolithography instead of E-beam lithography for the typical design rule of ring filters. KOH silicon etching can also adjust not only the resonance frequencies but also coupling coefficients with a small sacrifice of guiding loss.

©2009 Optical Society of America

OCIS codes: (230.7390) waveguides, planar; (130.3120) Integrated optics devices; (130.7408) Wavelength filtering devices.

References and links

1. H. Rong, S. Xu, Y. H. Kuo, V. Sih, O. Cohen, O. Raday, and M. Paniccia, "Low-threshold continuous-wave Raman silicon laser," Nat. Photonics **1**(4), 232–237 (2007).
2. Q. Xu, B. Schmidt, S. Pradhan, and M. Lipson, "Micrometre-scale silicon electro-optic modulator," Nature **435**(7040), 325–327 (2005).
3. J. B. You, M. Park, J. W. Park, and G. Kim, "12.5 Gbps optical modulation of silicon racetrack resonator based on carrier-depletion in asymmetric p-n diode," Opt. Express **16**(22), 18340–18344 (2008).
4. Q. Xu, B. Schmidt, J. Shakya, and M. Lipson, "Cascaded silicon micro-ring modulators for WDM optical interconnection," Opt. Express **14**(20), 9431–9435 (2006).
5. Y. Vlasov, W. M. J. Green, and F. Xia, "High-throughput silicon nanophotonic wavelength-insensitive switch for on-chip optical networks," Nat. Photonics **2**(4), 242–246 (2008).
6. T. Barwicz, M. A. Popović, P. T. Rakich, M. R. Watts, H. A. Haus, E. P. Ippen, and H. I. Smith, "Microring-resonator-based add-drop filters in SiN: fabrication and analysis," Opt. Express **12**(7), 1437–1442 (2004).
7. S. Xiao, M. H. Khan, H. Shen, and M. Qi, "A highly compact third-order silicon microring add-drop filter with a very large free spectral range, a flat passband and a low delay dispersion," Opt. Express **15**(22), 14765–14771 (2007).
8. A. Melloni, "Synthesis of a parallel-coupled ring-resonator filter," Opt. Lett. **26**(12), 917–919 (2001).
9. B. E. Little, S. T. Chu, P. P. Absil, J. V. Hryniewicz, F. G. Johnson, F. Seiferth, D. Gill, V. Van, O. King, and M. Trakalo, "Very High-Order Microring Resonator Filters for WDM applications," IEEE Photon. Technol. Lett. **16**(10), 2263–2265 (2004).
10. F. Xia, M. Rooks, L. Sekaric, and Y. Vlasov, "Ultra-compact high order ring resonator filters using submicron silicon photonic wires for on-chip optical interconnects," Opt. Express **15**(19), 11934–11941 (2007).
11. J. M. Lee, S. Park, and G. Kim, "Multichannel silicon WDM ring filters fabricated with DUV lithography," Opt. Commun. **281**(17), 4302–4306 (2008).
12. S. Xiao, M. H. Khan, H. Shen, and M. Qi, "Multiple- channel silicon micro-resonator based filters for WDM applications," Opt. Express **15**(12), 7489–7498 (2007).
13. F. Xia, L. Sekaric, M. O'Boyle, and Y. Vlasov, "Coupled resonator optical waveguides based on silicon-on-insulator photonic wires," Appl. Phys. Lett. **89**(4), 041122 (2006).
14. J. K. S. Poon, J. Scheuer, Y. Xu, and A. Yariv, "Designing coupled-resonator optical waveguide delay lines," J. Opt. Soc. Am. B **21**(9), 1665–1673 (2004).
15. Q. Li, Z. Zhang, F. Liu, M. Qiu, and Y. Su, "Dense wavelength conversion and multicasting in a resonance-split silicon microring," Appl. Phys. Lett. **93**(8), 081113 (2008).
16. Q. Xu, V. R. Almeida, and M. Lipson, "Micrometer-scale all-optical wavelength converter on silicon," Opt. Lett. **30**(20), 2733–2735 (2005).
17. J. Niehusmann, A. Vörckel, P. H. Bolivar, T. Wahlbrink, W. Henschel, and H. Kurz, "Ultrahigh-quality-factor silicon-on-insulator microring resonator," Opt. Lett. **29**(24), 2861–2863 (2004).

#111888 - $15.00 USD Received 26 May 2009; revised 25 Jun 2009; accepted 25 Jun 2009; published 29 Jun 2009

18. S. Xiao, M. H. Khan, H. Shen, and M. Qi, "Compact silicon microring resonators with ultra-low propagation loss in the C band," Opt. Express **15**(22), 14467–14475 (2007).
19. M. S. Nawrocka, T. Liu, X. Wang, and R. R. Panepucci, "Tunable silicon microring resonator with wide free spectral range," Appl. Phys. Lett. **89**(7), 071110 (2006).
20. Q. Xu, D. Fattal, and R. G. Beausoleil, "Silicon microring resonators with 1.5-microm radius," Opt. Express **16**(6), 4309–4315 (2008).
21. W. R. Headley, G. T. Reed, S. Howe, A. Liu, and M. Paniccia, "Polarization-independent optical racetrack resonators using rib waveguides on silicon-on-insulator," Appl. Phys. Lett. **85**(23), 5523 (2004).
22. J. M. Lee, D. J. Kim, G. H. Kim, O. K. Kwon, K. J. Kim, and G. Kim, "Controlling temperature dependence of silicon waveguide using slot structure," Opt. Express **16**(3), 1645–1652 (2008).
23. M. A. Popovic, C. Manolatou, and M. R. Watts, "Coupling-induced resonance frequency shifts in coupled dielectric multi-cavity filters," Opt. Express **14**(3), 1208–1222 (2006).
24. T. Naganawa, H. Haeiwa, and Y. Kokubun, "UV-induced refractive index change of SiN film and its application to center wavelength trimming of vertically coupled microring resonator filter," Jpn. J. Appl. Phys. **43**(No. 8B), 5780–5784 (2004).
25. Technology paper LETI_03, Jan. 5. 2009, *http://www.epixfab.eu/uploads/media/Technology_LETI_03.pdf.*

1. Introduction

Silicon microring resonators have attracted a lot of attention to be applied to various photonic devices, Raman silicon lasers [1], ring modulators [2–4], add-drop switches [5–7], MUX/DeMUX ring filters [8–12], optical buffers [13,14], wavelength converters [15,16], and sensors [17], which include almost all of the optical devices required for the on-chip photonic networks. Such versatility of the silicon ring resonators is owing to the properties of high refractive index contrast, optical resonance with a high quality factor, and transparency to off-resonance light without intrinsic reflection. To enhance characteristics of ring devices, various studies have been conducted and reported on low loss rings, high quality factors, large free spectral ranges (FSR), and polarization independency [18–21].

Despite the efforts, fundamental difficulties still remain including temperature-dependent resonance frequency shift, coupling-induced resonance frequency shift (CIFS), avoiding E-beam lithography, polarization dependency of ring characteristics, and statistical variations of channel wavelengths. A study to reduce temperature-dependent resonance frequency shifts has been reported with −2 pm/0°C [22]. Authors in Ref. 23 suggest theoretically that coupling-induced resonance frequency shift can be corrected by pre-distorting the resonance frequencies of coupled rings. The most untreatable problem is the process-induced statistical variation of resonance frequency which introduces serious obstacles for ring filters and modulators to be applied to photonic devices. Although the resonant frequency trimming had been tried with UV irradiation on Polymer or SiN waveguide rings [24], to our knowledge, neither significant theoretical studies nor experiments to reduce the process-induced statistical variation of the resonant frequencies of Si-waveguide rings have been reported, though it is the most serious hinderer in implementing the photonic interconnects. The process-induced statistical variation of the resonant frequencies not only induces deviations of channel frequencies which make the ring devices incompatible with other frequency-designated elements, but it also severely distorts spectral shapes of high order ring filters.

It is shown that the process-induced statistical variation of resonance frequency can be reduced significantly by introducing a nitride (Si_3N_4, refractive index n = 2.0) layer on the core waveguides or by KOH silicon etching. Etching the nitride layer shifts the resonance frequencies and reshapes the transmitted spectra without introducing an extra loss or extra variations of channel spacing. The nitride layer increases the smallest gap in the coupling regions from 100 nm to >150 nm which is larger than the minimum spacer width 120 nm or the guaranteed width 160 nm for the ArF photolithography [25]. The resonance frequencies and coupling coefficients between rings and bus lines can also be adjusted by KOH wet-etching with a small sacrifice of guiding loss.

2. Process-induced statistical variation of resonance wavelength

To estimate the seriousness of the process-induced statistical variation of resonance frequencies, ring resonators prepared by three different facilities were compared, ArF (193 nm) photolithography at LETI via ePIXfab in Europe, E-beam lithography at the KAIST

#111888 - $15.00 USD Received 26 May 2009; revised 25 Jun 2009; accepted 25 Jun 2009; published 29 Jun 2009
(C) 2009 OSA

nano-fab center and Hg I-line photolithography at ETRI both in KOREA. The etching processes were carried out by the same facilities where the lithography processes were taken place. First, for ArF photolithography, a typical variation range of the resonance wavelength for a selected 1st order 8-channel filter, which was reported in Ref. 11, is more than ± 0.5 nm. Second, for E-beam lithography, a typical variation range of ± 1.55 nm was measured for the 1st order 8-channel ring filter selected as one of best chips.

Figure 1(a) shows the transmission spectra of 1st order 8-channel ring resonators which were produced by the Hg I-line photolithography and reactive ion etching (RIE) with inductively coupled plasma (ICP) source. The statistical variation of the resonance wavelengths is shown in Fig. 1(b) for 6 chips, 48 channels, collected around the center of a processed SOI wafer. The channel spacing between adjacent channels was measured and plotted for the histogram of the number of channels. The mean value of the channel spacing is 1.152 nm and a standard deviation from the mean value is σ = 0.58 nm. The measured ring resonators have a radius of 4.25 μm, a waveguide width of 500 nm, and the gap size in the coupling region of 150 nm, which was formed by double-exposed lithography.

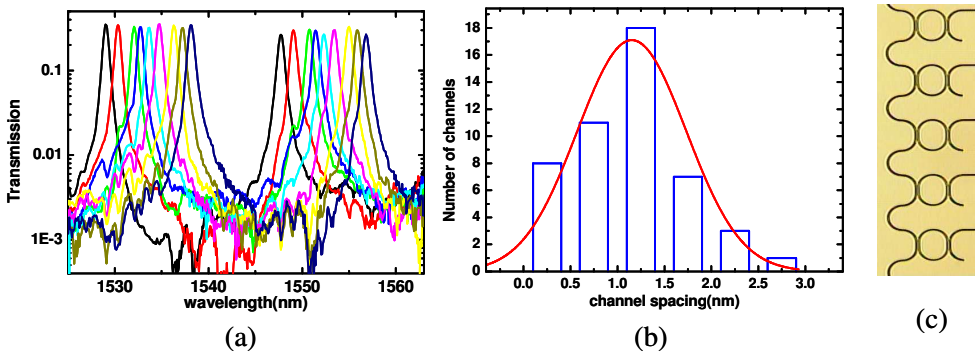

Fig. 1. (a) Transmission spectra of 1st order 8-channel ring resonators produced by the Hg I-line photolithography, where different color curves represent different channels. (b) Statistical variation of the resonance wavelengths. (c) Microscope image of 1st order ring resonators.

To estimate how seriously the typical variation of ± 0.5 nm deteriorates ring resonator filters, the transmission spectra of 3rd and 5th order ring resonators are calculated in Fig. 2 and Fig. 3, using the transfer matrix Eqs. (13),

$$\begin{bmatrix} a_{n+1} \\ b_{n+1} \end{bmatrix} = (\mathbf{PQ})^n \mathbf{P} \begin{bmatrix} a_0 \\ b_0 \end{bmatrix} \tag{1}$$

$$\mathbf{P} \equiv \begin{bmatrix} -\dfrac{r}{it} & \dfrac{1}{it} e^{-jkL_c} \\ -\dfrac{1}{it} e^{jkL_c} & \dfrac{r}{it} \end{bmatrix} \tag{2}$$

$$\mathbf{Q} \equiv \begin{bmatrix} 0 & \alpha^{1/2} e^{jk(L_p/2)} \\ \alpha^{-1/2} e^{-jk(L_p/2)} & 0 \end{bmatrix}, \tag{3}$$

where L_c is the length of coupling region, L_p the length of ring periphery, r and t the cross-coupling and self-coupling coefficients in the coupling region, α the intensity attenuation factor of the ring. For 3rd order rings and no add signals, we have $n = 3$, $a_0 = 1$, $a_{n+1} = 0$. The transmission intensity of a signal through a channel port is given by $(b_{n+1})^2$.

#111888 - $15.00 USD Received 26 May 2009; revised 25 Jun 2009; accepted 25 Jun 2009; published 29 Jun 2009
(C) 2009 OSA

As the resonant wavelengths of three rings are in accordance, the transmission spectrum has a nice flat top shape with a bandwidth of 1.48 nm and out-of-band rejection ratio of more than 40 dB, as shown in Fig. 2(a), where the coupling coefficient for the bus lines and the side rings is $r^2 = 0.3$ and that for the side rings and the center ring is $r^2 = 0.03$ with the attenuation factor $\alpha = 0.995$. As the resonant wavelength of the center ring is shifted to 1550.5 nm and that of either side ring to 1549.5 nm, varied by 0.5 nm longer and shorter, the transmission spectrum is severely deteriorated, as shown in Fig. 2(b), by more than 10 dB height of a spiky peak which makes the filter unusable.

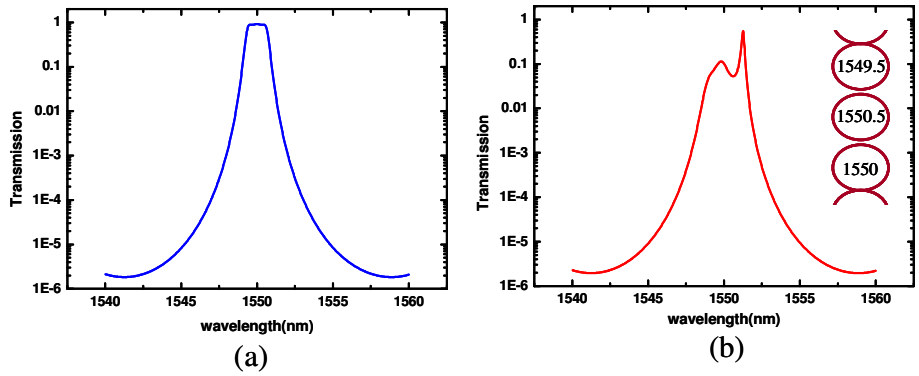

Fig. 2. Transmission spectra of 3rd order rings of which resonance wavelengths are, (a) in perfect accordance, (b) varied by 0.5 nm longer and shorter, as shown in the inset.

The variation of resonance wavelength for the 5th order rings makes a much worse effect on the transmission spectrum in the drop port as shown in Fig. 3, where the wavelengths of either two adjacent rings among three in the center shift to 1550.5 nm and 1549.5 nm with others being 1550 nm. Abnormal peaks destroy the spectrum by more than 25 dB, which, if no variation, should be a very ideal shape for filters. The coupling coefficients, 0.3, 0.03, 0.02 in order from bus lines, have been used for the calculations.

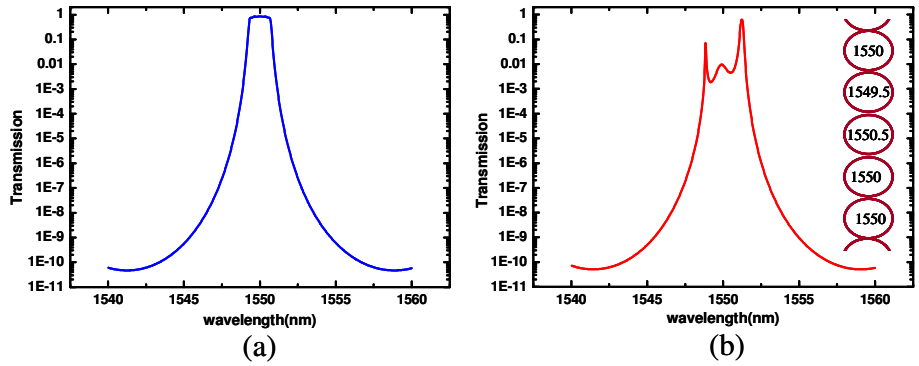

Fig. 3. Transmission spectra of 5th order rings of which resonance wavelengths are, (a) in perfect accordance, (b) varied by 0.5 nm longer and shorter, as shown in the inset.

3. Adjusting resonance wavelength using a SiN layer

Figures 4(a) and 4(b) show the transmission spectra of 3rd order ring resonator filters before and after depositing a SiN layer, where the red curves represents theoretical modeling calculated using transfer matrix method and the black curves represents experimental

#111888 - $15.00 USD Received 26 May 2009; revised 25 Jun 2009; accepted 25 Jun 2009; published 29 Jun 2009
(C) 2009 OSA

measurements. A 6" SOI wafer with 260 nm thick silicon layer on a 2 μm buried oxide layer was used to prepare the samples. The radius of the ring is 4.25 μm, and the waveguide width is 0.5 μm, which were patterned by E-beam lithography. FSR and the group index were measured 17.76 nm and n_g = 4.405. The 5th order rings are unrealistically difficult to predict and correct their statistical irregularities. Here we focus on the 3rd order rings because their theoretical specifications are above the levels required for the WDM filter.

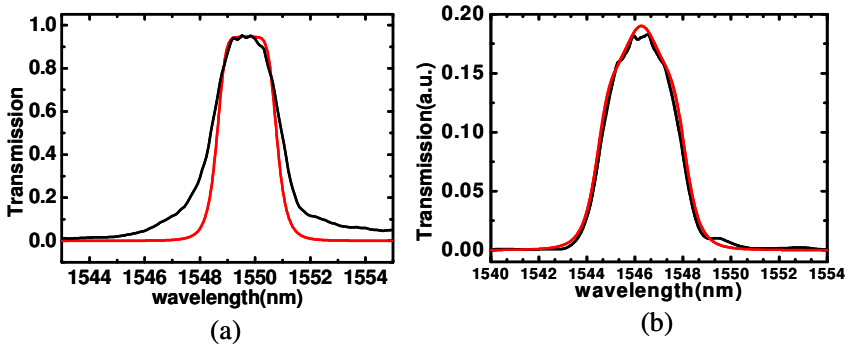

Fig. 4. Transmission spectra of 3rd order rings (a) before and (b) after depositing 4000 Å thick SiN, red curves for theoretical calculations and black for experiments.

The coupling coefficients r^2 to produce the spectrum shown in Fig. 4(a) are 0.5 for the coupling between side rings and bus lines with 2 μm long MMI, and 0.07 for the coupling between the side rings and the center ring with 2 μm long straight waveguides separated by 100 nm gap. The intensity attenuation factor α is 0.995 for a single pass of the ring perimeter. After measuring the spectrum of Fig. 4(a), the same ring resonators were used to coat 4000 Å thick LPCVD Si_3N_4, which causes to change the transmission spectra as shown in Fig. 4(b). The coupling coefficients increase from 0.5 to 0.6 for the MMI and from 0.07 to 0.15 for the 100 nm gap. The spectral bandwidth increases from 2.64 nm to 3.32 nm due to the higher refractive index of SiN in the coupling regions.

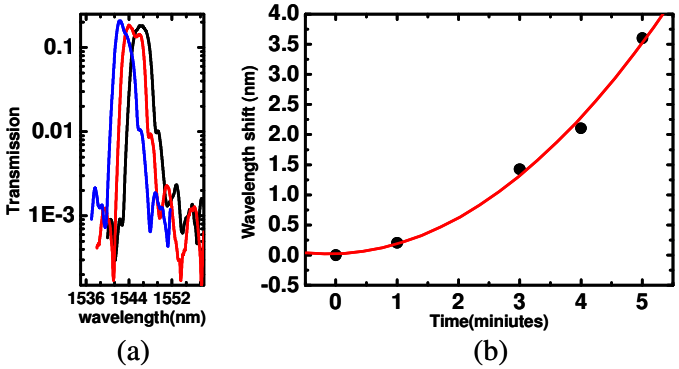

Fig. 5. shows the shifts of (a) spectral curves for the etched times of 0, 3, 5 minutes and (b) resonant wavelengths as the thickness of the SiN varied, where 1 min corresponds to 500 Å decrease.

The thickness of the nitride layer was varied by reactive ion etching (RIE). The etching rate was 500 Å per minute, approximately. Figure 5(a) shows the measured spectra for etched times of 0, 3, 5 minutes. As the thickness of the cladding nitride layer decreases, the group refractive index of the waveguide n_g decreases, and the optical length of the ring periphery also decreases to shift the resonant frequency to the shorter wavelength. Our measurement

#111888 - $15.00 USD Received 26 May 2009; revised 25 Jun 2009; accepted 25 Jun 2009; published 29 Jun 2009
(C) 2009 OSA

showed that the frequency shifts were so uniform for whole 8 channels that channel spacing was not changed. As shown in the Fig. 5(a), there is no difference in the transmitted intensities between 0 and 5 min etchings or 3.6 nm shift which is large enough to shift misaligned center frequencies of the filter to pre-designated values. The spectral shape is also unchanged, effectively. Figure 5(b) shows the frequency shift as a function of the etched time. The curved line is for eye–guidance. As expected, the resonant wavelength moves in such a predicted way that an accurate amount of wavelength can be displaced with a pre-experimental data.

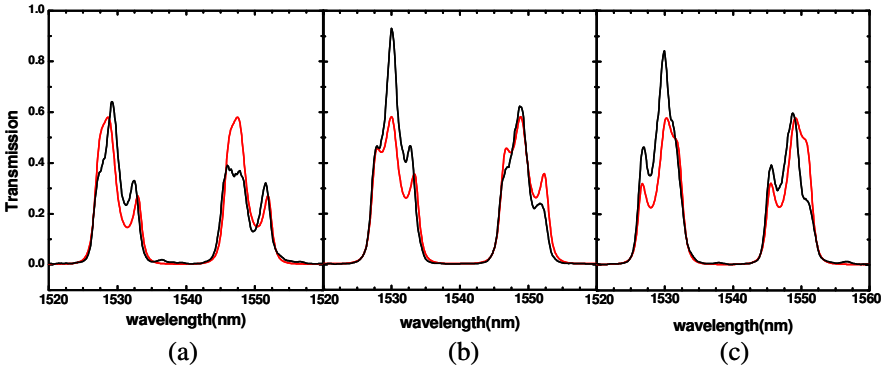

Fig. 6. Transmission spectra of 3rd order ring filters (a) before RIE and after (b) 30s x3 and (c) 30s x5 RIE for the center ring, red curves for theoretical calculations and black for experiments.

Figure 6 shows the experimental and theoretical curves of spiky peaks due to mismatch of resonant wavelengths for 3rd order rings. The spectral curves were measured from a different channel of the same filter used in Fig. 5. After 4 etchings to obtain graphs in Fig. 5(b), the same filter was used in the experiment of Fig. 6 to reshape their spiky curves. A contact aligned photolithography was used to open the center ring with side rings covered by photo-resist. The cladding nitride layer on the center ring was etched by RIE for five 30 seconds steps.

Figure 6(a) shows a spectrum measured before RIE, showing two transmission bands spaced by free spectral range and broadened due to the nitride layer. From theoretical fit, we found that the 3rd order rings are very attractive for a potential device because all peaks can be identified and fit theoretically by adjusting the parameters, resonant wavelengths of the rings, coupling coefficients, and the loss factor, in Eqs. (1)-(3). One aspect of the 3rd order ring is that the resonant wavelengths of two side rings are in good accordance, as expected from symmetry, while that of the center ring is shifted to shorter or longer wavelength. The spectrum in Fig. 6(a) shows that the resonance wavelength of the center ring is longer by 3.2 nm than those of the side rings. We attribute the shift of resonance wavelength of center ring with respect to those of the side rings to the coupling-induced resonance frequency shift in addition to process-induced statistical errors.

As the nitride layer on the center ring is etched away by 30s x3 in Fig. 6(b), and 30s x5 in Fig. 6(c), the peak of center ring moves in a predicted way toward the shorter wavelength. The side lobes at 1530 nm and 1550 nm transmission bands are minimized at the time of 30s x4 etchings. Figure 6 also shows an interesting fact that output intensities haven't changed before and after etching the center ring for 150 sec.

To find an appropriate gap size of the coupling region which was covered by a nitride layer, we measured transmission spectra of 1st order ring in Fig. 7, which was located side by side at the same wafer and prepared by the same process as the 3rd order rings. The upper curve is for air cladding and 100 nm gap, and the lower curve for nitride cladding and 150 nm gap between the ring and bus lines. All parameters except the gap sizes are exactly the same

#111888 - $15.00 USD Received 26 May 2009; revised 25 Jun 2009; accepted 25 Jun 2009; published 29 Jun 2009
(C) 2009 OSA

for both rings. The quality factor for air cladding and 100 nm gap was measured Q = 3875 at 1550 nm, and that for nitride cladding and 150 nm gap was measured Q = 2422 at 1557 nm, which proves that the corresponding required gap size is lager than 150 nm which makes the ArF photolithography possible and also proves that the bending loss with radius of 4.25 μm is not so high to allow the specification of the filters.

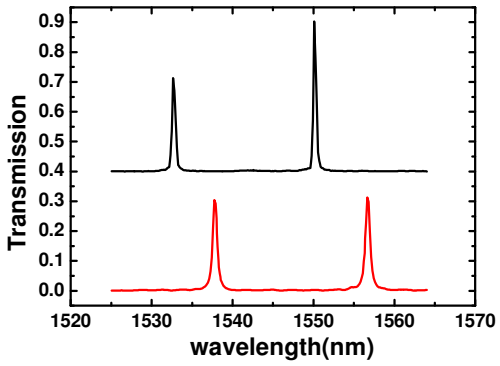

Fig. 7. Transmission spectra of 1st order rings, upper curve for air clad and 100 nm gap and lower curve for nitride clad and 150 nm gap.

4. KOH wet-etching of Si waveguides

The procedure to etch Si crystals by KOH solution is well known in many literatures. The etch rate is strongly dependent on the crystal directions, according to which the side wall of a waveguide patterned along (110) plane is etched in such a shape as shown in Fig. 8(a). The (110) plane has the highest etch rate, while the (111) plane has the smallest rate, which results in the angle 35.26° between the horizontal and the (111) planes. A SEM image of an etched waveguide is shown in Fig. 8(b). As the sidewalls of waveguides in coupling regions are aligned with the (110) planes, the coupling coefficients can be adjusted to a smaller value by an application of KOH solution.

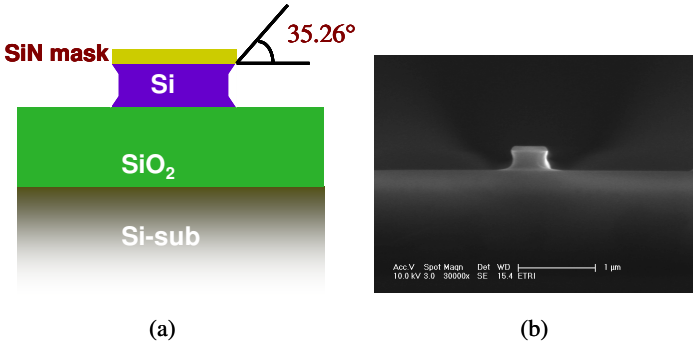

Fig. 8. (a) a schematic diagram to etch a Si waveguide by KOH solution and (b) a SEM image of the etched waveguide.

The 45% solution of KOH at 85 °C was used to etch 3rd order ring resonators for 5 sec to bring the effects on the spectrum in Fig. 9. As expected from the reduced coupling, the spectral bandwidth decreases from 2.46 nm to 2.11 nm. The resonance wavelength red shifts from 1537.1 nm to 1535.8 nm due to the narrower width of the waveguide which causes a smaller group refractive index. One weak point is that the transmitted power decreases by 10%, approximately, mainly due to the increased propagation loss caused by the geometrical

#111888 - $15.00 USD Received 26 May 2009; revised 25 Jun 2009; accepted 25 Jun 2009; published 29 Jun 2009
(C) 2009 OSA

profile of the side walls. As the sample was etched by some more time, the transmitted power was reduced to lower than 50%, which means that the profile of the side wall is inadequate for a waveguide. At 85 °C, the etch rate is quite fast and sensitive to the small change of temperature, which makes a small adjustment of the spectrum difficult. It is desirable to carry out the etching at a strictly stabilized and a little lower temperature to achieve an accurate adjustment.

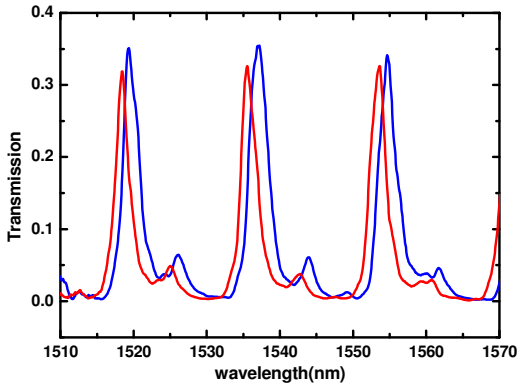

Fig. 9. Transmission spectra of a 3rd order ring resonator before and after etching the Si waveguide for 5 sec by KOH solution

5. Conclusion

The two critical problems in the silicon ring resonators, process-induced statistical errors of resonance wavelengths and utilizing photolithography instead of E-beam lithography, can be relieved by a simple way of depositing a cladding silicon nitride layer on the rings. It is shown that a layer of 4000 Å thick Si_3N_4 can adjust resonance wavelengths of whole channels uniformly or individually, and reshape their spectral curves for 3rd order rings. It is also verified that the nitride layer changes the coupling coefficients in such a way that the minimum size of the gap in the coupling region allows the ArF photolithography instead of E-Beam lithography. Since the procedure to deposit or etch the nitride layers has been established well in CMOS process, our experiment can be applicable immediately to any CMOS compatible processes. The 45% solution of KOH at 85 °C was used to etch the side wall of 3rd order ring resonators to adjust not only the resonance wavelengths but also the coupling strengths. It showed that etching for 5 sec changed the spectral bandwidth by 0.35 nm and the resonance wavelength by 1.3 nm.

Acknowledgements

This work was supported by the Ministry of Knowledge Economy of the Korean Government. The Authors acknowledge the colleagues in National NanoFab Center, KAIST, for their helps to prepare samples.

#111888 - $15.00 USD Received 26 May 2009; revised 25 Jun 2009; accepted 25 Jun 2009; published 29 Jun 2009
(C) 2009 OSA